

Supporting Information for

***The Cobalt Hydride that Never Was: Revisiting Schrauzer's "Hydridocobaloxime"***

David C. Lacy, Gerri M. Roberts, Jonas C. Peters\*

Division of Chemistry and Chemical Engineering, California Institute of Technology, Pasadena, CA 91125, United States

E-mail: jpeters@caltech.edu

<b>Contents</b>	<b>Page</b>
Crystallography	S2
Table S1. Crystallography	S2
General & Synthetic Methods	S3
Figure S1. Variable temperature NMR spectrum of [ <b>P-Co<sup>II</sup></b> ] <sub>2</sub>	S5
Figure S2. SQUID data for [ <b>P-Co<sup>II</sup></b> ] <sub>2</sub>	S6
Figure S3. Variable temperature UV-vis of [ <b>P-Co<sup>II</sup></b> ] <sub>2</sub> in toluene	S7
Figure S4. EPR spectrum of [ <b>P-Co<sup>II</sup></b> ] <sub>2</sub> in toluene at RT and 77K	S8
Figure S5. NMR spectrum of [ <b>P-Co<sup>II</sup></b> ] <sub>2</sub> from [Co <sup>II</sup> (dmgH) <sub>2</sub> (OH <sub>2</sub> )]	S8
Figure S6. <sup>1</sup> H-NMR spectrum of [ <b>P-Co<sup>II</sup></b> ] <sub>2</sub> from CoCp <sub>2</sub> reduction	S9
Figure S7. <sup>1</sup> H-NMR spectrum of [ <b>P-Co<sup>II</sup></b> ] <sub>2</sub> with -5 ppm resonance	S10
Figure S8. <sup>1</sup> H-NMR spectrum of [ <b>P<sub>2</sub>Co<sub>3</sub></b> ] in d <sub>6</sub> .benzene	S11
Figure S9. FAB-MS(+) of [ <b>P<sub>2</sub>Co<sub>3</sub></b> ]	S12
Figure S10. SQUID data for [ <b>P<sub>2</sub>Co<sub>3</sub></b> ]	S13
Figure S11. FTIR spectra of [ <b>P<sub>2</sub>Co<sub>3</sub></b> ], [ <b>P-Co<sup>II</sup></b> ] <sub>2</sub> , and [ <b>P-Co<sup>III</sup>Cl</b> ]	S14
Figure S12. UV-vis and <sup>1</sup> H-NMR spectrum of [ <b>P-Co<sup>II</sup></b> ] <sub>2</sub> + 1 atm H <sub>2</sub>	S15
Figure S13. CV of [ <b>P-Co<sup>II</sup></b> ] <sub>2</sub> in DCM	S16

## Crystallography

*General Methods.* XRD data were collected on either a Bruker D8 Venture kappa duo photon 100 cmos instrument or a Siemens or Bruker three-circle diffractometer with a Smart 1K CCD detector using Mo K $\alpha$  radiation ( $\lambda = 0.71073$ ), performing  $\phi$ - and  $\omega$ -scans and cooled with an Oxford Cryosystems crystal cooling system. The structures were solved by direct methods and refined on F<sup>2</sup> by full-matrix least-squares techniques using SHELX program package<sup>2,3,4</sup> and Olex2.<sup>1,2</sup> For both structures, the hydrogen atoms were added at calculated positions and refined upon with a riding model. For the [P-Co<sup>II</sup>]<sub>2</sub> structure refinement, the butyl carbon atoms not attached to phosphorus were highly disordered across two positions and were not refined anisotropically. The refinement of the [P-Co<sup>II</sup>]<sub>2</sub> structure is poor and gives rise to the high weighted values. These two issues (disordered butyl groups and high weighted values) cause the level B alerts in the check cif. Improvement was not possible despite attempts on three different sets of crystals grown from various evaporations of toluene, benzene, or methylcyclohexane; the same poor refinement was obtained. Nonetheless, the structure clearly shows that a cobalt ion is bonded to two [dmgH]<sup>-</sup> ligands and one phosphine ligand and is in close proximity to another cobalt ion of the same ligation. The unit cell for [P<sub>2</sub>Co<sub>3</sub>]•dmgH<sub>2</sub> contained an uncoordinated dmgH<sub>2</sub> unit and formed a close contact H-bond interaction between the OH group of dmgH<sub>2</sub> and an oxygen atom on [P<sub>2</sub>Co<sub>3</sub>].

**Table S1.** Crystal data and structure refinement for the two cobalt complexes.

formula	[P-Co <sup>II</sup> ] <sub>2</sub> C <sub>40</sub> H <sub>82</sub> Co <sub>2</sub> N <sub>8</sub> O <sub>8</sub> P <sub>2</sub>	[P <sub>2</sub> Co <sub>3</sub> ]•dmgH <sub>2</sub> C <sub>48</sub> H <sub>94</sub> Co <sub>3</sub> N <sub>12</sub> O <sub>12</sub> P <sub>2</sub>
FW	982.93	1270.09
T (K)	100	100
crystal system	Monoclinic	Triclinic
space group	P2 <sub>1</sub> /c	P -1
a (Å)	15.069(3)	12.4969(8)
b (Å)	10.049(2)	13.0533(9)
c (Å)	17.288(3)	19.965(2)
$\alpha$ (deg)	90	108.231(3)
$\beta$ (deg)	111.795(5)	90.429(3)
$\gamma$ (deg)	90	93.880(3)
Z	2	2
V (Å <sup>3</sup> )	2430.7(7)	1270.09
d <sub>calcd</sub> (Mg/m <sup>3</sup> )	1.343	1.363
Indep. Reflections	5517	26515
R1	0.1465	0.0593
wR2	0.4145	0.1737
GOF	1.054	1.029

## Physical and Synthetic Methods

All reagents were purchased from commercial sources and used as received unless otherwise noted. Compounds were manipulated under inert atmosphere using an N<sub>2</sub>-filled M-Braun glove box or using standard Schlenk line techniques. Literature methods were followed for the preparation of [Cl-Co<sup>III</sup>(dmgH)<sub>2</sub>(pyridine)] and [Cl-Co<sup>III</sup>(dmgH)<sub>2</sub>P(nBu)<sub>3</sub>].<sup>3</sup> Solvents were sparged with nitrogen and dried over columns containing molecular sieves or alumina. The deuterated solvents were degassed and dried over activated 3-Å sieves prior to use. NMR spectra were recorded on Varian 300 MHz, 400 MHz, and 500 MHz spectrometers. <sup>1</sup>H chemical shifts are reported in ppm relative to residual solvent as internal standards and are singlets unless otherwise stated. Electronic absorbance spectra were recorded with a Cary 50 spectrometer. Fourier transform infrared ATR spectra were collected on a Thermo Scientific Nicolet iS5 Spectrometer with diamond ATR crystal (utilized iD5 ATR insert). High-res fast atom bombardment (FAB) spectra were collected on a JMS-600H High Resolution Mass Spectrometer. X-band EPR spectra were recorded on a Bruker EMX spectrometer. EPR simulations were performed using *SpinCount*, which was written by and obtained from Prof. Michael P. Hendrich.<sup>4</sup> In order to obtain a reasonable fit for the trimer, the transitions from both m<sub>s</sub> states (|±1/2⟩ & |±3/2⟩) were included. Magnetic susceptibility measurements were obtained using a Quantum Designs SQUID magnetometer running MPMSR2 software. SQUID samples were loaded in polycarbonate capsules and suspended in plastic straws and transferred from the glove box into a liquid nitrogen dewar before placing them in the SQUID. SQUID samples were then centered at 35 K using a DC centering scan at 500 gauss.

*Reduction of [Cl-Co<sup>III</sup>(dmgH)<sub>2</sub>P(nBu)<sub>3</sub>] with NaBH<sub>4</sub> for the Preparation of [P-Co<sup>II</sup>]<sub>2</sub> and [P<sub>2</sub>Co<sub>3</sub>].* Literature methods were used with slight modifications.<sup>5</sup> [Cl-Co<sup>III</sup>(dmgH)<sub>2</sub>P(nBu)<sub>3</sub>] (1.000 g, 1.900 mmol) was suspended in 50 mL of an aqueous methanol buffer (1:1) with 1.166 g tribasic phosphate and 0.638 g of monobasic phosphate and adjusted such to achieve a pH 7 solution. The suspension of [Cl-Co<sup>III</sup>(dmgH)<sub>2</sub>P(nBu)<sub>3</sub>] was degassed with N<sub>2</sub>. In a separate flask, NaBH<sub>4</sub> (0.303 g, 8.010 mmol) was dissolved with 5 mL of degassed H<sub>2</sub>O via cannula under an N<sub>2</sub> atmosphere. The NaBH<sub>4</sub> solution was added dropwise *via* syringe over a 20-minute period, which caused the solution to bubble and form a black-purple precipitate and a blue solution (the UV-vis spectrum of the blue solution has bands at 620 nm, 398 nm, and a shoulder at 286 nm). The purple solid was isolated on a swivel frit on a Schlenk line with positive N<sub>2</sub> pressure. The purple solid was washed with degassed water one time (the blue filtrate slowly turned orange when stored under N<sub>2</sub> and was discarded) and subsequently dried overnight at room temperature on the Schlenk line. Afterwards, the crude material was brought into a glove box and isolated in a tared vial (0.5 g, crude product). Slow evaporation of a concentrated benzene solution of the crude material yielded black needles suitable for X-ray diffraction. Extracting with several 10 mL portions of pentane and passing the solutions through Celite purified the crude material from brown impurities. The purple pentane filtrates were combined and reduced to dryness. This process was repeated until no solid material remained upon extraction with pentane and eventually yielded 300 mg (32%) of [P-Co<sup>II</sup>]<sub>2</sub>. Material used for SQUID measurements was recrystallized by storing a saturated pentane solution [P-Co<sup>II</sup>]<sub>2</sub> at -35 °C, decanting, and subsequently washing the purple solid with cold hexamethyldisiloxane one time. Characterization of [P-Co<sup>II</sup>]<sub>2</sub>. <sup>1</sup>H-NMR (toluene-*d*<sub>8</sub>, 500 MHz, -91 °C): δ 18.23 (2H, s, OH), δ 2.59 (12H, s, CH<sub>3</sub>), δ 1.13 (6H, s, CH<sub>2</sub>), δ 0.88 (15H, t, J = 7.1 Hz, CH<sub>2</sub>CH<sub>3</sub>), δ 0.75 (6H, s, CH<sub>2</sub>). <sup>31</sup>P-NMR (toluene-*d*<sub>8</sub>, 202 MHz, -91 °C): δ -2.41 ppm. Solid ATR-FTIR, Figure S11. UV-vis, Figure S3. Anal Calcd. (found) for [P-Co<sup>II</sup>]<sub>2</sub>, C<sub>40</sub>H<sub>82</sub>Co<sub>2</sub>N<sub>8</sub>O<sub>8</sub>P<sub>2</sub>: %C 48.88 (48.78); %H 8.41 (8.54); %N 11.40 (11.33).

The material that was left behind from the pentane extractions (described above) was a brown solid. This material was dissolved in benzene and passed through Celite pad and the filtrate was lyophilized to yield 130 mg of the [P<sub>2</sub>Co<sub>3</sub>] trimer (17%). <sup>1</sup>H-NMR (benzene-*d*<sub>6</sub>, 400 MHz, RT) δ -21.89, δ -6.11, δ -0.26, δ 14.47, δ 24.36, δ 33.18, δ 40.56. <sup>1</sup>H-NMR (MeCN-*d*<sub>3</sub>, 400 MHz, RT): δ -22.04, δ -5.06, δ 0.40, 16.23, δ 25.73, δ 33.11, δ 40.39. 77 K X-band EPR spectrum is silent. 10 K

X-band EPR spectrum contains an 8-line pattern centered at  $g = 7.9$  ( $a = 740$  MHz) and broad feature at  $g = 1$  (see Figure 6 of the text for simulation parameters). High-res FAB-MS(+)  $m/z_{(found)} = 1153.397$ ;  $m/z_{(calcd)} = 1153.400$ .

*Preparation of  $[Co^{II}(dmgH)_2P(nBu)_3]_2$  via  $CoCp_2$ .*  $[Cl-Co^{III}(dmgH)_2P(nBu)_3]$  (14.9 mg, 0.028 mmol) starting material and cobaltocene (5.2 mg, 0.028 mmol) were stirred in about 5 mL of benzene for 1.5 h. A pale green precipitate was removed by filtering over Celite. The product was then lyophilized. (12.3 mg, 88%). The  $^1H$ -NMR spectrum in  $d_6$ -benzene was identical to the material prepared from  $NaBH_4$  reductions. A crystal with identical unit-cell parameters as those obtained for  $[P-Co^{II}]_2$  was obtained by slow evaporation of benzene solution of the compound into methylcyclohexane.

*Preparation of  $[Co^{II}(dmgH)_2P(nBu)_3]_2$  via addition of phosphine to  $[Co^{II}(dmgH)_2(OH_2)_2]$ .* Solid  $[Co^{II}(dmgH)_2(OH_2)_2]$  was prepared by a method described by Norton & coworkers.<sup>6</sup> A 16 mL DCM suspension of  $[Co^{II}(dmgH)_2(OH_2)_2]$  (400 mg, 1.23 mmol) was treated with  $PnBu_3$  (247 mg, 1.23 mmol) dropwise via a syringe. The solution rapidly turned dark purple and was stirred for 30 min. The dimer  $[P-Co^{II}]_2$  was isolated by removing the DCM solvent *in-vacuo* and washing the solid with 10 mL pentane and filtering through Celite. The pentane filtrate was concentrated to dryness to yield a purple solid (520 mg, 87%). The  $^1H$ -NMR was identical to  $[P-Co^{II}]_2$  prepared by  $NaBH_4$  (See Figure S5); albeit the product is not very clean as the monomer complex  $[P-Co^{II}]$  reacts with alkyl halides. Smaller quantities of analytically pure material can be alternatively prepared in pentane. The phosphine (27 mg, 0.13 mmol, 0.9 equiv.) in 1 mL of pentane was added to a suspension of  $[Co^{II}(dmgH)_2(OH_2)_2]$  (50 mg, 0.15 mmol) in 5 mL pentane and stirred for 4 hours, filtered through Celite, and the filtrate concentrated to obtain the purple solid in 70% yield. The  $^1H$ -NMR was identical to  $[P-Co^{II}]_2$  prepared by  $NaBH_4$  (See Figure S11). Anal Calcd. (found) for  $[P-Co^{II}]_2$ ,  $C_{40}H_{82}Co_2N_8O_8P_2$ : %C 48.88 (48.74); %H 8.41 (8.51); %N 11.40 (11.36).

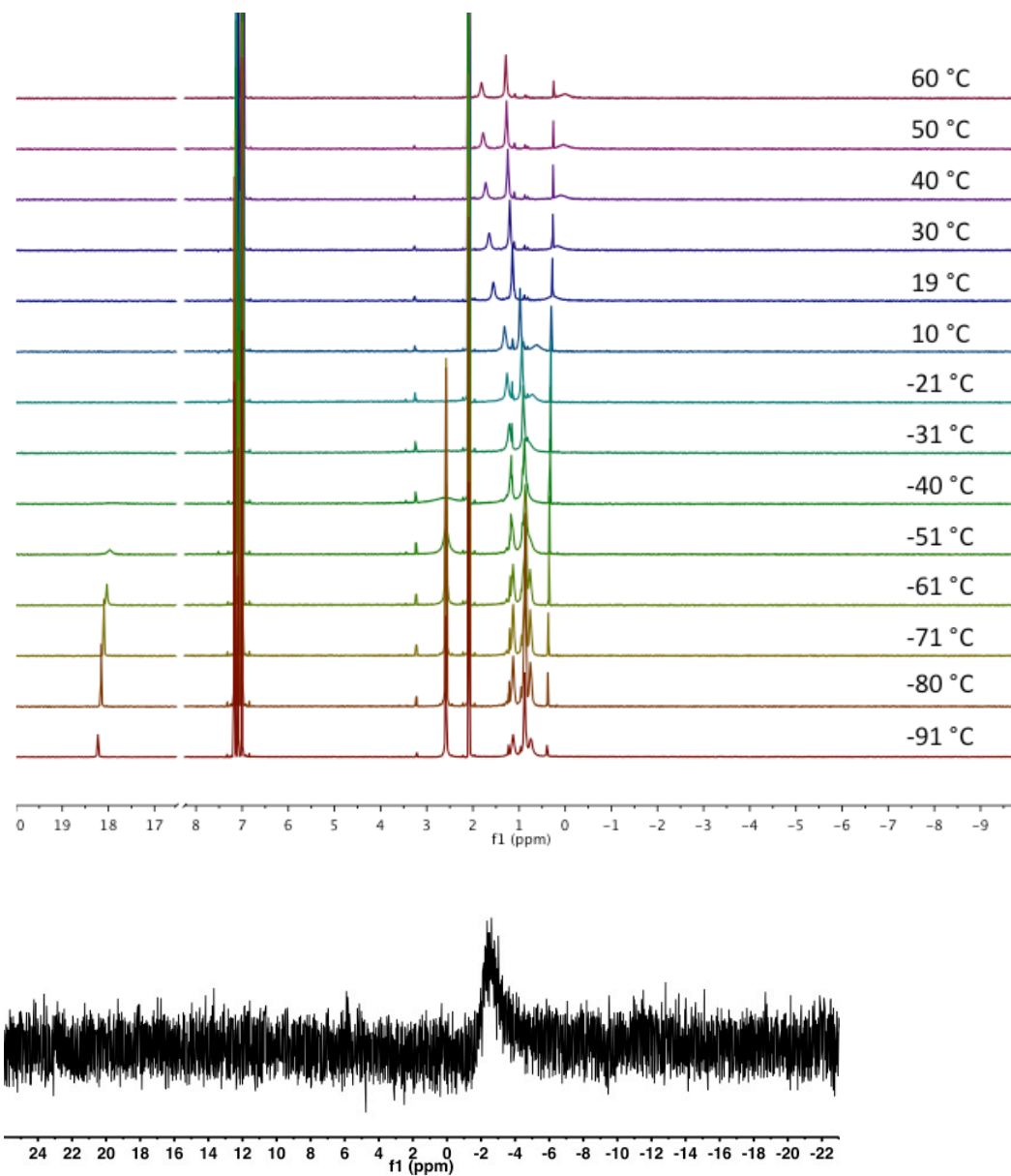


**Figure S1.** (top) Variable temperature  $^1\text{H}$ -NMR spectra of  $[\text{P-Co}^{\text{II}}]_2$  in  $d_8$ -toluene. All resonances from the range of -45 to 45 ppm are displayed. (bottom)  $^{31}\text{P}$ -NMR spectrum of  $[\text{P-Co}^{\text{II}}]_2$  in  $d_8$ -toluene collected at -91 °C.

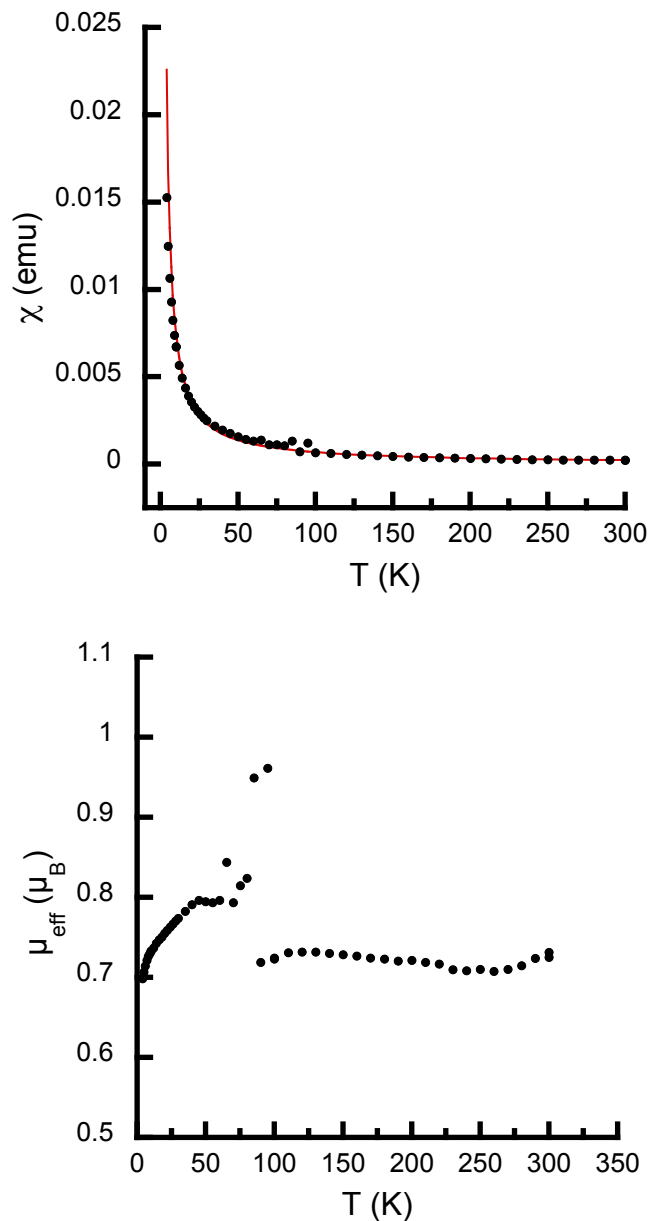


**Figure S2.** (top) A plot of the magnetic susceptibility,  $\chi$  (emu), vs. T (K) for  $[\mathbf{P-Co}^{\text{II}}]_2$  collected at 1 tesla using a super conducting quantum interference device (SQUID). The fit (red) was performed using the program Julx version 1.4.1.<sup>7</sup> A diamagnetic correction was applied using Pascal's constants<sup>8</sup> for the molecule and for the sample holder for the fit. The model for the fit required the inclusion of a spin 3/2 paramagnetic impurity ( $4.3\% \pm 0.6$ , three samples); modeling the data as a doublet or a ferromagnetically or antiferromagnetically coupled system did not provide reasonable fits.  $^1\text{H-NMR}$  & EPR (10 K) spectra collected after the SQUID measurement confirmed small amounts of  $[\mathbf{P}_2\text{Co}_3]$  ( $S = 3/2$ ) in the sample. Parameters:  $g = 2$ ,  $\Theta_W = 6.320$ . (bottom) A plot of the magnetic moment,  $\mu_{\text{eff}}$  ( $\mu_B$ ) vs. T (K) for  $[\mathbf{P-Co}^{\text{II}}]_2$  collected at 1 tesla. The anomalous rise at  $\sim 100$  K was reproducible across three samples and may arise from the fact that in the range of 50 - 100 K, the raw data crosses zero magnetic moment (essentially no magnetic measurement) and could not be fit by the software interfaced with the SQUID.

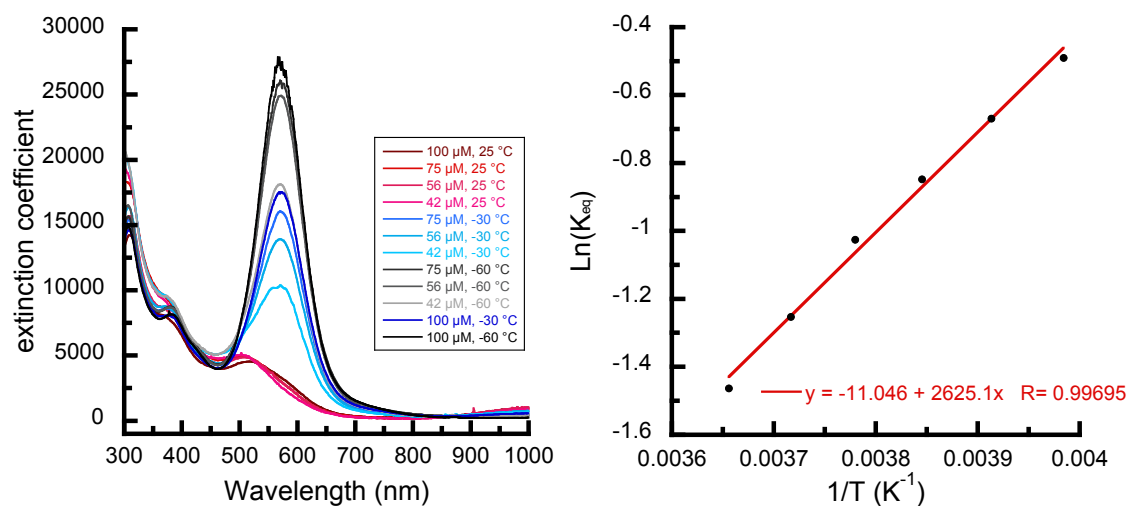


**Figure S3a.** (Left) UV-vis spectrum of  $[\text{P-Co}^{\text{II}}]_2$  in toluene at 25 °C (red), -30 °C (blue) and -60 °C (black/grey) at four different concentrations plotted against supposed extinction coefficient (1 cm cell). At higher temperatures (60 °C – 100 °C) the monomeric species does not absorb at 750 nm and thus the extinction coefficient could be determined for the dimer (750 nm,  $1010 \text{ M}^{-1} \text{ cm}^{-1}$ ). (Right) A Van't Hoff plot was constructed monitoring the 750 nm band in the temperature range of -5 °C to -30 °C using 5 degree increments (measurement performed in triplicate with 300  $\mu\text{M}$   $[\text{P-Co}^{\text{II}}]_2$  solutions in a 1 cm cell).

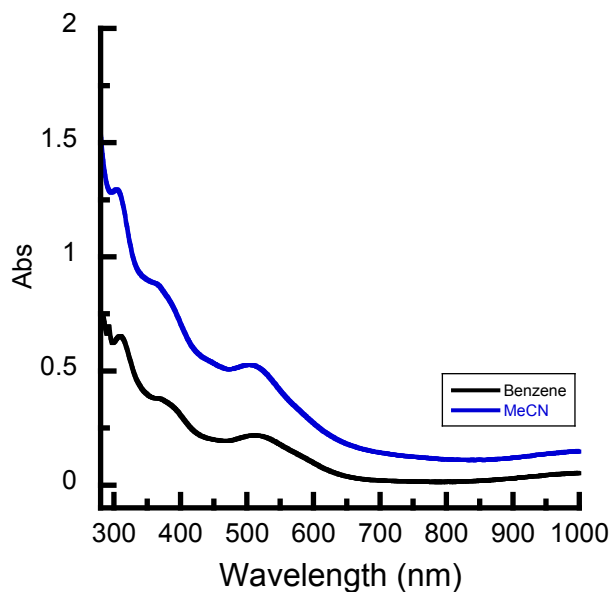


**Figure S3b.** UV-vis spectrum of  $[\text{P-Co}^{\text{II}}]_2$  in benzene (black) and MeCN (blue) at RT (conc.  $\sim 50 \mu\text{M}$ ).

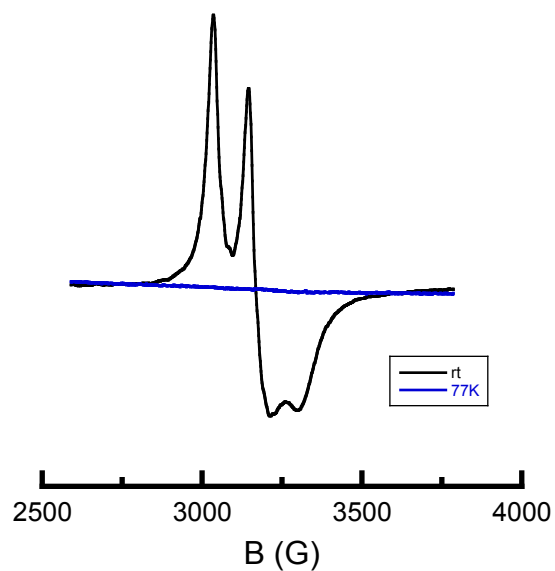


**Figure S4.** EPR spectra of 2.0 mM  $[\mathbf{P-Co}^{\text{II}}]_2$  in toluene at RT (black) and 77 K (blue).

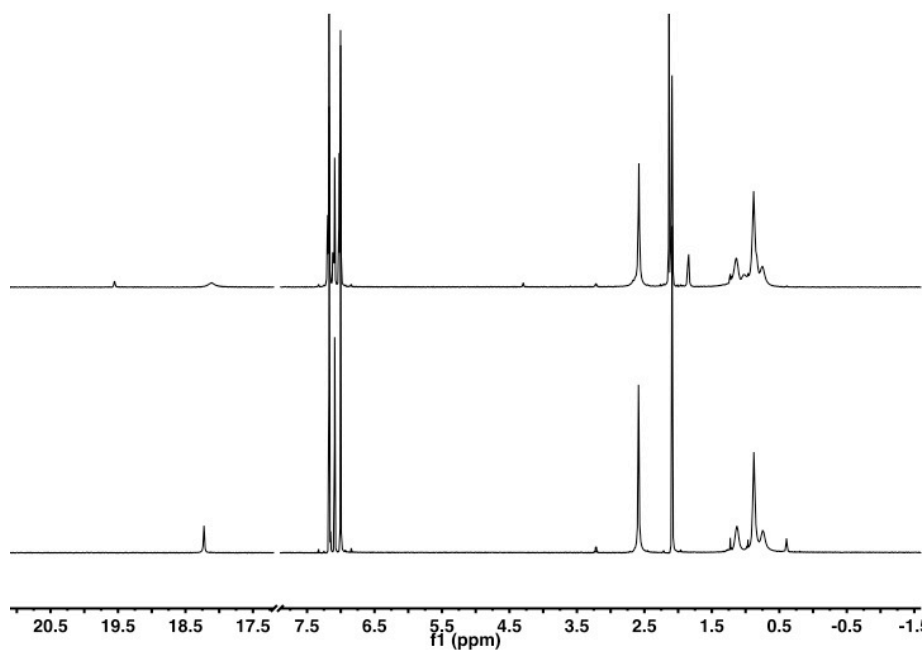


**Figure S5a.**  $^1\text{H-NMR}$  spectrum of  $[\mathbf{P-Co}^{\text{II}}]_2$  in  $d_8$ -toluene at  $-91\text{ }^\circ\text{C}$  prepared by treatment of  $[\text{Co}^{\text{II}}(\text{dmgH})_2(\text{OH})_2]$  with  $\text{P}(n\text{Bu})_3$  in DCM (top) compared to the  $-91\text{ }^\circ\text{C}$  spectrum of  $[\mathbf{P-Co}^{\text{II}}]_2$  in  $d_8$ -toluene prepared from  $\text{NaBH}_4$  reduction (bottom). For the product synthesized by addition of phosphine in DCM, at least one additional compound is present, apparent by the feature at 19.5 ppm.

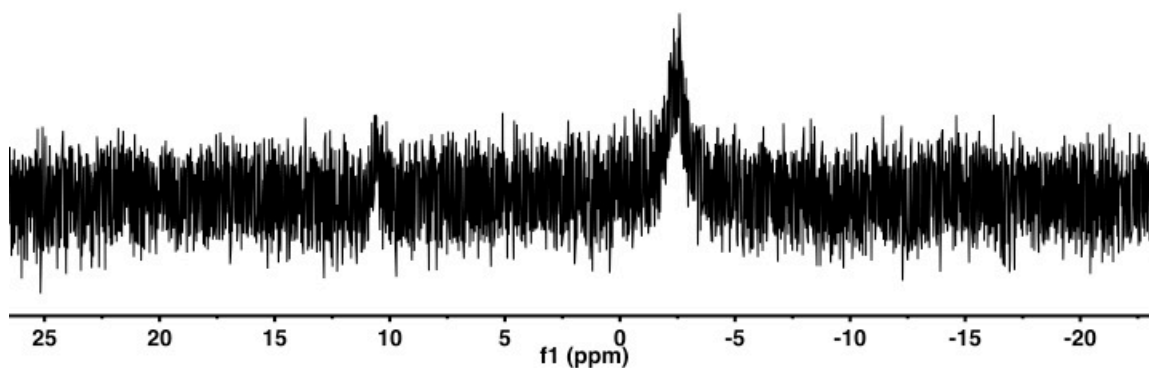


**Figure S5b.**  $^{31}\text{P}$ -NMR spectrum of  $[\text{P-Co}^{\text{II}}]_2$  in  $d_8$ -toluene at  $-91\text{ }^\circ\text{C}$  prepared by treatment of  $[\text{Co}^{\text{II}}(\text{dmgH})_2(\text{OH})_2]$  with  $\text{P}(n\text{Bu})_3$  in DCM. The  $[\text{P-Co}^{\text{II}}]_2$  compound prepared by this method contains at least one other species, as evident by the feature at 10 ppm in the  $^{31}\text{P}$ -NMR. The feature at  $-2.5$  ppm matches the chemical shift seen from the  $\text{NaBH}_4$  reduction product (Figure S1).

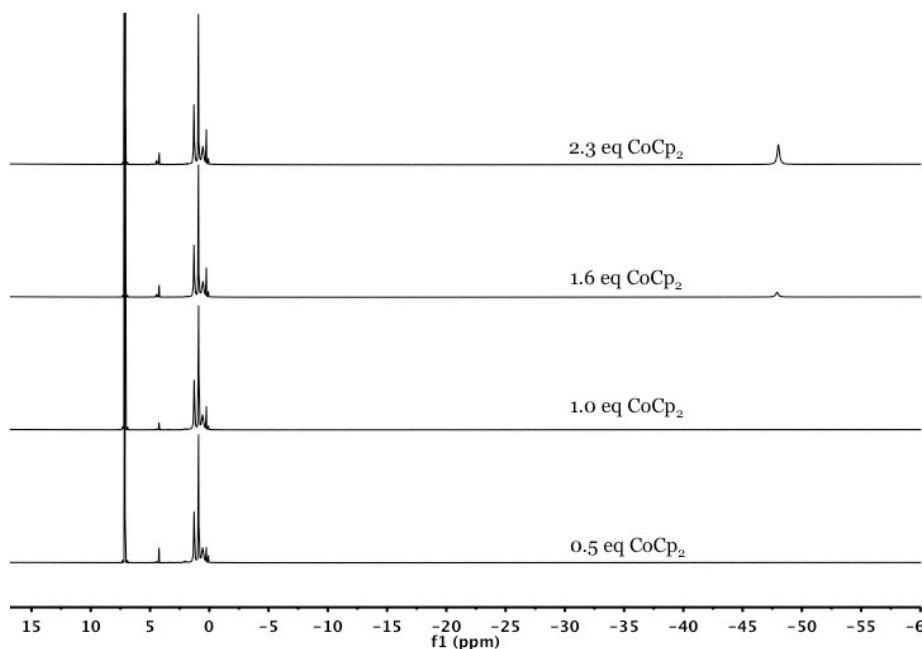


**Figure S6.**  $^1\text{H}$ -NMR spectrum of  $[\text{P-Co}^{\text{II}}]_2$  in  $d_6$ -benzene prepared by treatment of  $[\text{P-Co}^{\text{III}}\text{Cl}]$  with  $\text{CoCp}_2$  in  $\text{C}_6\text{H}_6$  and subsequent work-up by filtration and removal of solvent (feature at  $-48$  ppm is unreacted  $\text{CoCp}_2$ ). See figure S12 for CV of  $[\text{P-Co}^{\text{III}}\text{Cl}]$ . A crystal with identical unit-cell parameters to  $[\text{P-Co}^{\text{II}}]_2$  obtained from  $\text{NaBH}_4$  reduction was obtained from this  $\text{Cp}_2\text{Co}$  reduction.

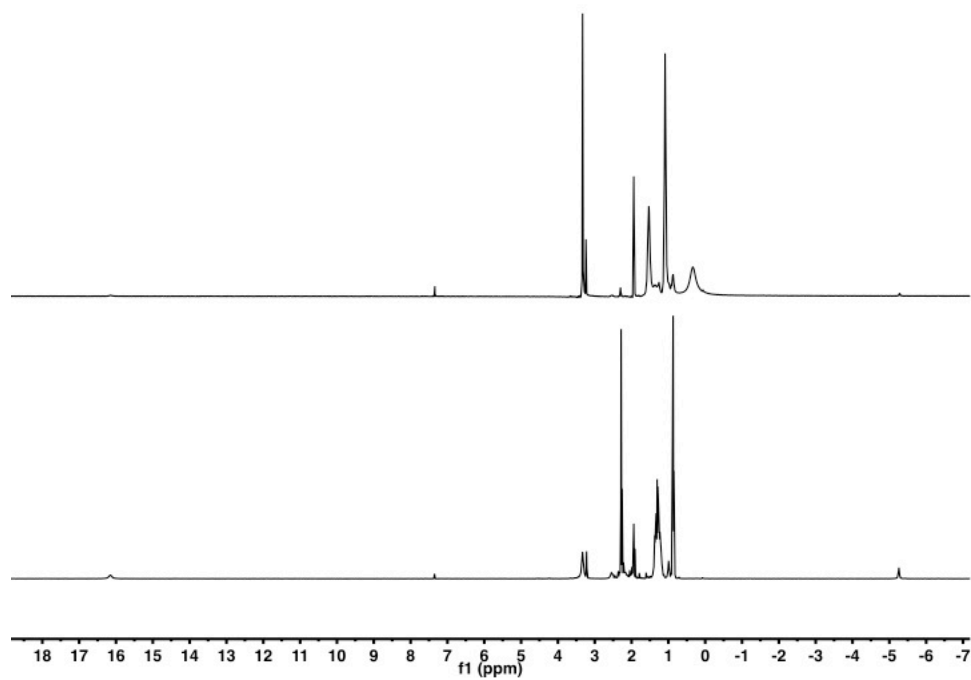


**Figure S7a.**  $^1\text{H}$ -NMR spectrum of  $[\text{P-Co}^{\text{II}}]_2$  in  $d_3$ -MeCN at RT before addition of air (top) and after addition of air (bottom). Some signal at -5 ppm is apparent before addition of air in this sample.

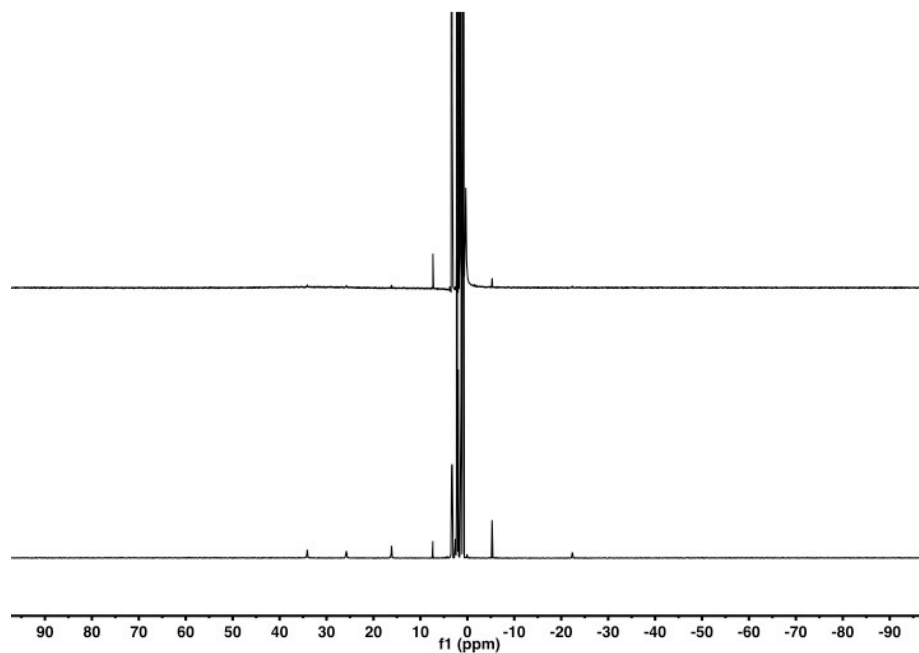


**Figure S7b.** Wide  $^1\text{H}$ -NMR spectrum of  $[\text{P-Co}^{\text{II}}]_2$  in  $d_3$ -MeCN at RT before addition of air (top) and after addition of air (bottom).

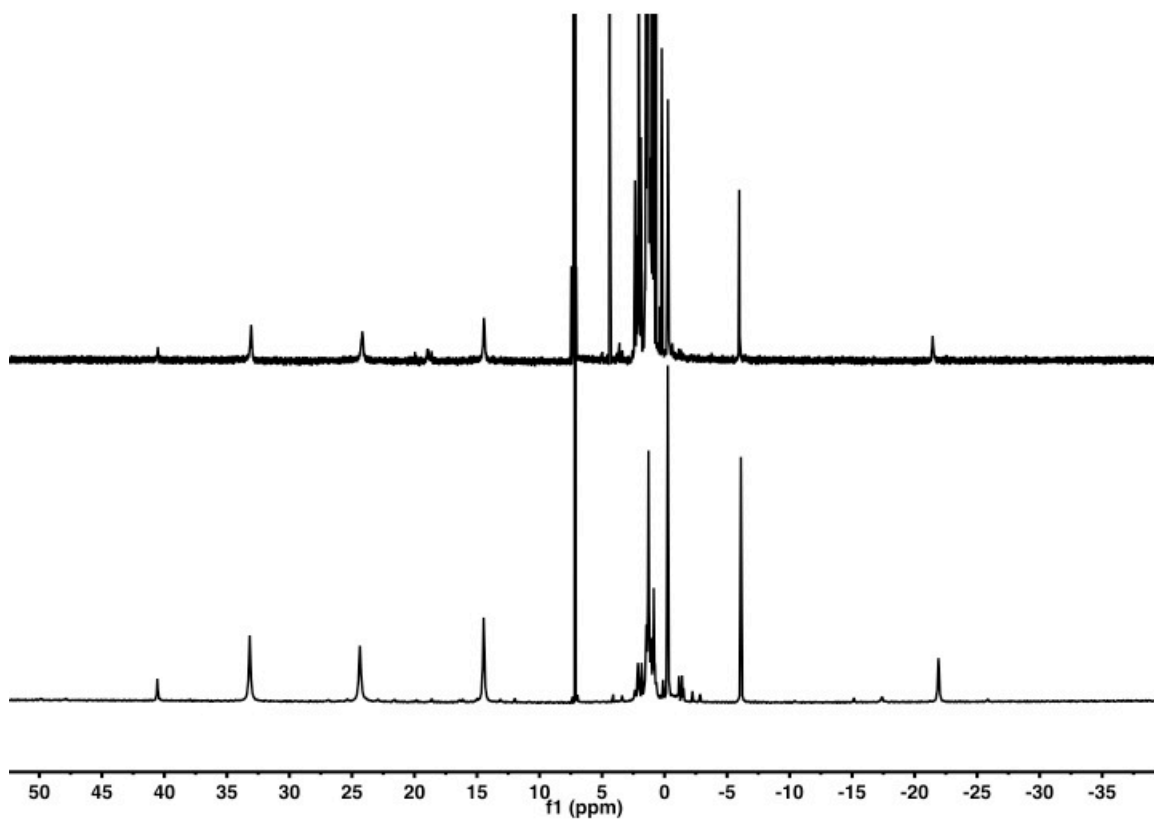


**Figure S8.**  $^1\text{H}$ -NMR spectrum of  $[\text{P}_2\text{Co}_3]$  in  $d_6$ -benzene as isolated from pentane washes of crude  $\text{NaBH}_4$  reaction (bottom) and the batch of crystals from which the molecular X-ray structure was obtained (top).

Scan: 2-3

Base: m/z 1153; 14.9%FS TIC: 1293064 (Max Inten : 155744)

Selected Isotopes : C H C<sub>0</sub>2<sub>3</sub>N<sub>9-11</sub>O<sub>9-11</sub>P<sub>2-3</sub>

Error Limit : 5 ppm

<u>Measured Mass</u>	<u>% Base</u>	<u>Formula</u>	<u>Calculated Mass</u>	<u>Error</u>
1153.397	100.0%	C <sub>44</sub> H <sub>86</sub> C <sub>0</sub> 3N <sub>10</sub> O <sub>10</sub> P <sub>2</sub>	1153.400	-2.5

Scan: 2-3

Base: m/z 1153; 14.9%FS

TIC: 1293064 (Max Inten : 155744)

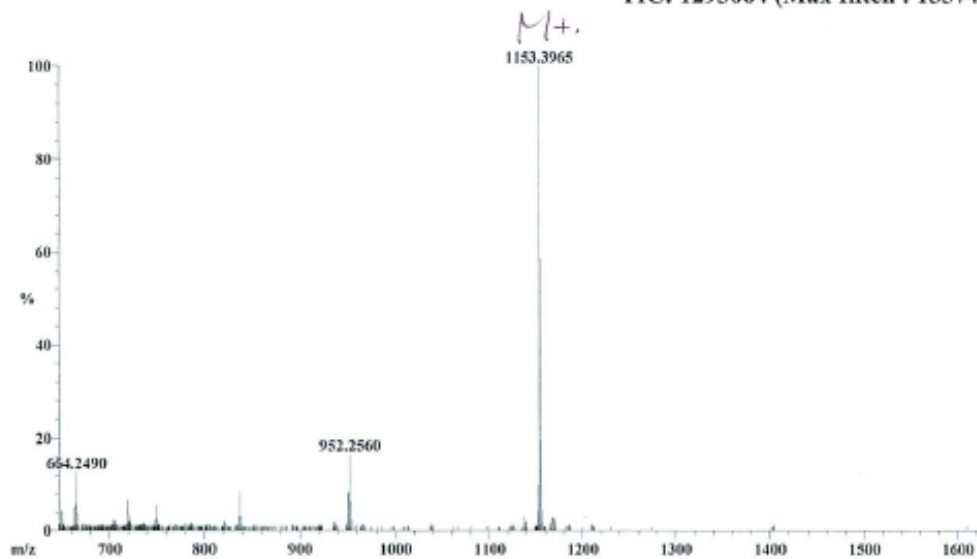
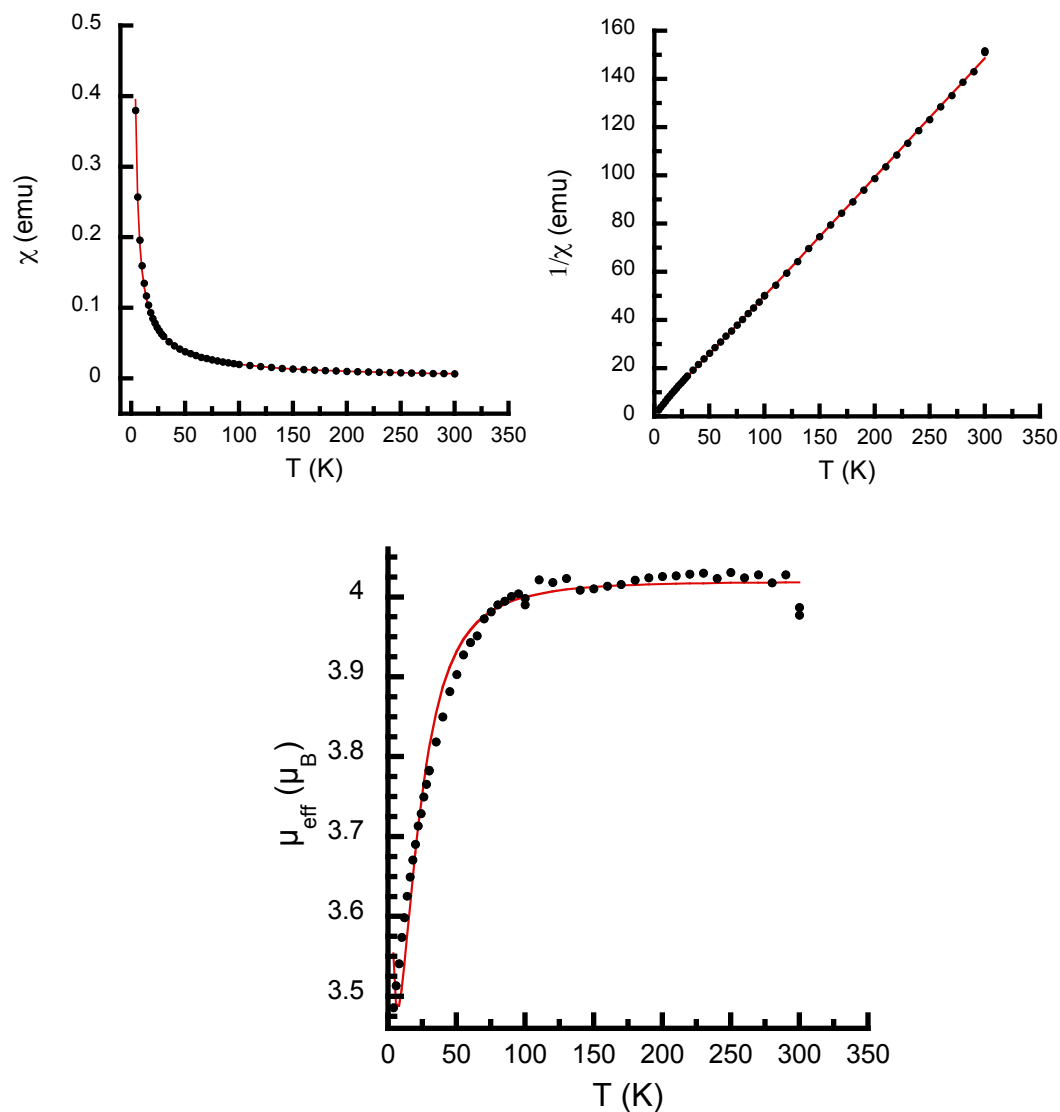
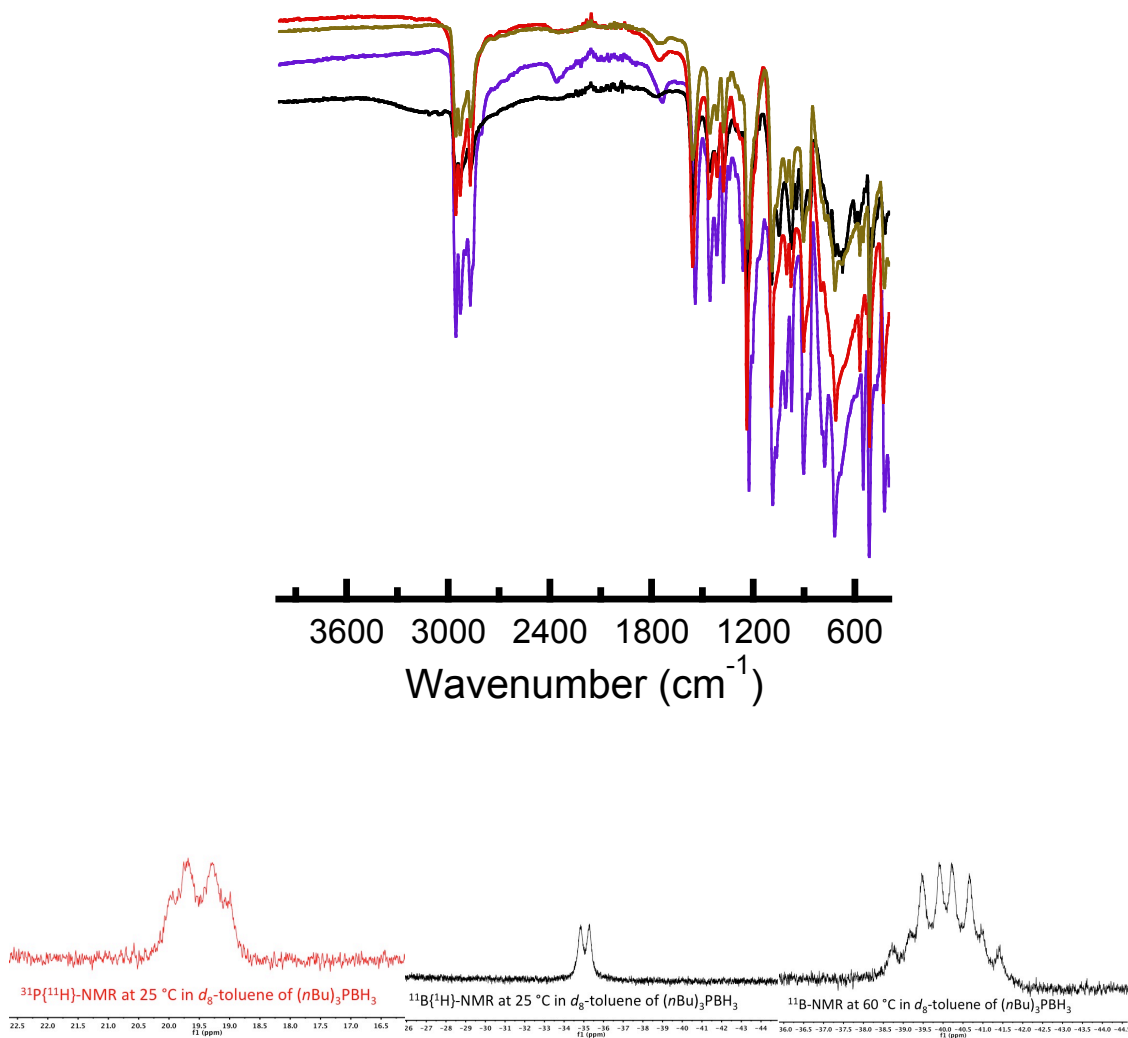


Figure S9. High-res FAB-MS(+) spectrum of [P<sub>2</sub>Co<sub>3</sub>].



**Figure S10.** Plots of the magnetic susceptibility,  $\chi$  (emu) vs. T (K),  $1/\chi$  (1/emu) vs. T (K) and magnetic moment,  $\mu_{\text{eff}}$  ( $\mu_{\text{B}}$ ), vs. T (K) for  $[\text{P}_2\text{Co}_3]$  at 0.5 T obtained using a super conducting quantum interference device (SQUID). The fit (red) was performed using the program Julx version 1.4.1.7 A diamagnetic correction was applied using Pascal's constants<sup>8</sup> for the molecule and for the sample holder for the fit. Parameters:  $g = 2.074$ ,  $D = -11 \text{ cm}^{-1}$ ,  $\Theta_{\text{W}} = 0.787$ .



**Figure S11.** Top: Solid ATR-FTIR spectrum of  $[\mathbf{P}_2\mathbf{Co}_3]$  (Trimer, black),  $[\mathbf{P-Co}^{\text{III}}\text{Cl}]$  (red), and crude  $[\mathbf{P-Co}^{\text{II}}]_2$  synthesized from  $\text{NaBH}_4$  (purple). The features at  $1740\text{ cm}^{-1}$  are from the O-H $\cdots$ O vibration as described in the literature.<sup>9</sup> The feature  $2360\text{ cm}^{-1}$  is due to residual  $(n\text{Bu})_3\text{P-BH}_3$ , which could not be eliminated after successive washings (note: the peak at  $2360\text{ cm}^{-1}$  is absent from product obtained via the  $\text{CoCp}_2$  reduction (yellow)). Bottom:  $^{31}\text{P}$  (20 ppm) (red) and  $^{11}\text{B}$ -NMR (-40 ppm) (black) experiments of the crude  $[\mathbf{P-Co}^{\text{II}}]_2$  material explicitly show the presence of a phosphine-borane species.

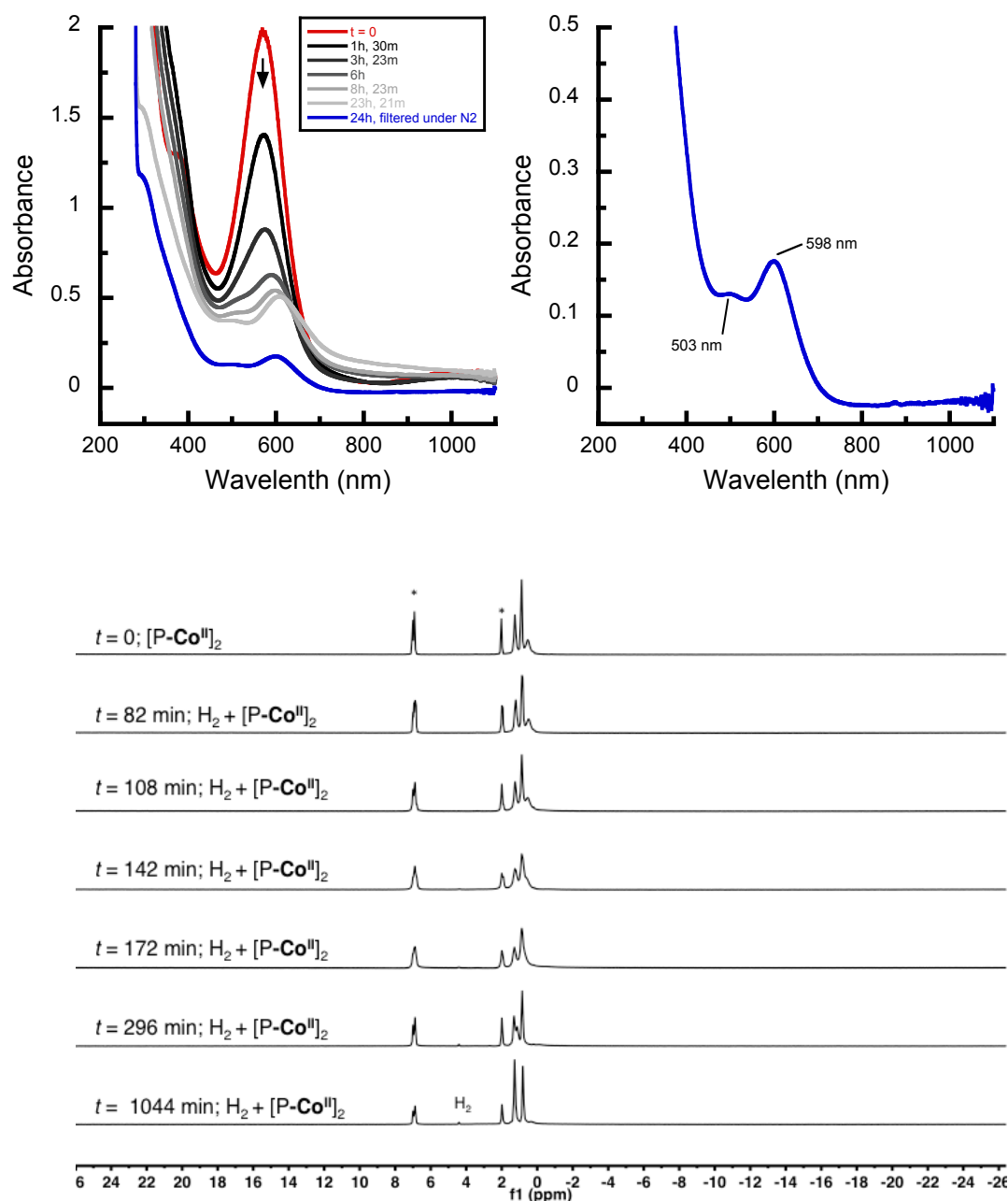


**Figure S12. (top)** UV-vis spectrum (1 mm path-length cell, RT) of 3.9 mM [P-Co<sup>II</sup>]<sub>2</sub> (solid red) plus 1 atm H<sub>2</sub> at room temperature in toluene. After 24 hours, the cell contained an appreciable amount of precipitate. The precipitate was removed by filtration in an N<sub>2</sub>-filled glovebox and the filtrate was transferred to the same, cleaned UV-Vis cell and its spectrum collected (blue spectrum top-right). **(bottom)** <sup>1</sup>H-NMR spectra before and after H<sub>2</sub> addition to 18 mM [P-Co<sup>II</sup>]<sub>2</sub> at RT in *d*<sub>8</sub>-toluene (\*) in a J-Young tube. The final spectrum remains unchanged after several days. Moreover, after several days the sample was subjected to three freeze-pump-thaw cycles and no change in the <sup>1</sup>H-NMR spectrum was observed (except that the resonance associated with H<sub>2</sub> disappears). No <sup>31</sup>P-NMR signals were found for any of these samples at RT.

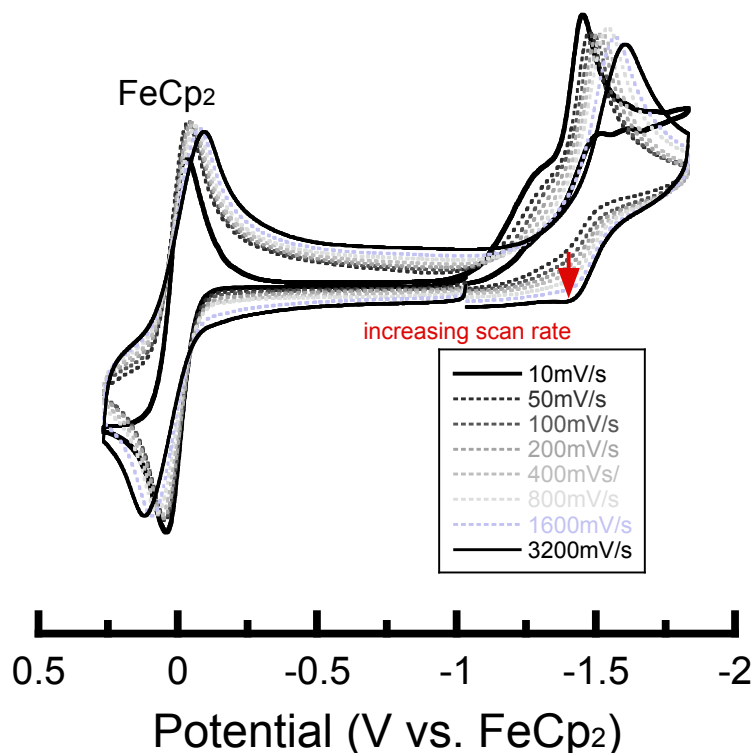


**Figure S13.** CV of [P-Co<sup>III</sup>Cl] in DCM with 0.1 M nBu<sub>4</sub>NPF<sub>6</sub> at various scan rates. The current was normalized by dividing the current by the square root of the scan rate. Conditions: concentration analyte = 0.5 mM; working and auxiliary electrode = glassy carbon; reference electrode = Ag wire with internal ferrocene (0.5 mM). Instrumentation: CH Instruments 630-C Electrochemical Analyzer with CHI Version 8.09 software package.

- (1) Sheldrick, G. M. *Acta. Cryst.* **2008**, A64, 112.
- (2) Dolomanov O.V., Blake A.J, Champness N.R., Schroder M. (2003). "OLEX: new software for visualization and analysis of extended crystal structures". *J. Appl. Cryst.***36**: 1283–1284.
- (3) (a) Kumar, K.; Gupta, B. *J. Organometallic Chem.* **2011**, 696, 3785. (b) Toscano, P. J.; Swider, T. F.; Marzilli, L. G.; Bresciani-Pahor, N.; Randaccio, L. *Inorg. Chem.* **1983**, 22, 3416.
- (4) Golombek, A. P.; Hendrich, M. P. J. *Magn. Reson.* 2003, 165, 33.
- (5) (a) Schrauzer, G. N.; Holland, *J. Am. Chem. Soc.* **1971**, 93, 1505. (b) Bhattacharjee, A.; Chavarot-Kerlidou, M.; Andreiadis, E. S.; Fontecave, M.; Field, M. J.; Artero, V. *Inorg. Chem.* **2012**, 51, 7087.
- (6) Li, G.; Han, A.; Pulling, M. E.; Estes, D. P.; Norton, J. R. *J. Am. Chem. Soc.* **2012**, 134, 14662.
- (7) *JulX* version: 1.4.1; magnetic susceptibility simulation software; Eckhard Bill: Max-Plank Institute, Germany **2008**.
- (8) Berry, J. F.; Bain, G. A. *J. Chem. Ed.* **2008**, 85, 532.
- (9) Yanazaki, N.; Hohokabe, Y. *Bull. Chem. Soc. Jpn.* **1971**, 44, 63.